Synthesis and Characterization of TEOS Coating Added With Innovative Antifouling Silica Nanocontainers and TiO$_2$ Nanoparticles

Ludovica Ruggiero[1]*, Maria Rosaria Fidanza*[1], *Morena Iorio*[2], *Luca Tortora*[1,2], *Giulia Caneva*[1], *Maria Antonietta Ricci*[1] *and Armida Sodo*[1]

[1] *Dipartimento di Scienze, Università degli Studi "Roma Tre", Rome, Italy,* [2] *Laboratorio Analisi Superfici, INFN Roma Tre, Rome, Italy*

We study the synthesis and characterization of an innovative TEOS-based composite coating, which could improve previous formulations used in the field of monument conservation. The proposed coating is composed by a tetraethoxyorthosilicate matrix (TEOS), containing an elasticiser [hydroxyl-terminated polydimethylsiloxane (PDMS-OH)] and a non-ionic surfactant (n-octylamine). The specific self-cleaning and antifouling properties are obtained by the addition of different kinds of nanofillers: the commercial TiO$_2$ nanoparticles, plus two different silica nanocontainers, loaded with the commercial biocide 2-mercaptobenzothiazole. Through a multi-analytical approach, we evaluate the effect of the nanoparticles concentration on the coatings drying rate, on the variation of their visual aspect and textural properties. Our results show that the addition of the silica nanocontainers at 0.05% (w/v) in sol does not change the color of the coating and reduces the formation of cracks after drying. Moreover, the coating charged with nanocontainers undergoes slower drying, thus improving its penetration into the pores of the treated surface. Further tests of photocatalytic and biocidal properties of this new product on different lithotypes and their potential interactions are in progress.

Keywords: multifunctional coating, TiO$_2$, SiO$_2$ nanocontainers, antifouling, biocide

INTRODUCTION

Most historical buildings and monuments, that are a seamless part of our urban landscape, employ natural and artificial stone materials, which are subject to deterioration processes, due to the interaction with the environment (Jackson et al., 2005; Bourges et al., 2008; Torraca, 2009; Doehne and Price Clifford, 2010). In particular, urban environment accelerates the deterioration and may cause crumble of outdoor surfaces (such as architectural elements and sculptures), due to pollution and high concentration of fine particulate. In addition, biotic factors, especially microorganisms, are among the main agents of stone damage (McNamara and Mitchell, 2005; Caneva et al., 2008; Scheerer et al., 2009). Given the large number and the different nature of the stone materials and the various related degradation processes, finding potential supporting solutions is a challenging issue.

Among the consolidant products used for stone, TEOS-based materials have relevant applications and properties (Kim et al., 2009; Zárraga et al., 2010). When these products are applied

on the decaying stone substrate, the tetraethoxysilane polymerizes into the porous structure, thus increasing the intragranular cohesion. Ideally, the TEOS matrix rebinds adjacent mineral grains (Zárraga et al., 2010), appreciably increasing the strength of the stone. However, although TEOS-based coatings are widely applied for consolidation interventions (Zárraga et al., 2010), it is well-known that during the drying phase these products undergo crack formation (Wen and Mark, 1995; Mosquera et al., 2003; Salazar-Hernández et al., 2009; Illescas and Mosquera, 2011; Xu et al., 2012; Pinho et al., 2013; Angulo-Olais et al., 2018).

Different authors have tested the effects of the addition of oxide nanoparticles. To quote a few of them, we mention that Milani et al. (2007) have investigated the realization of a new TEOS-based consolidant with colloidal silica particles. Kim et al. (2009) and the Mosquera's group (Mosquera et al., 2003) have also highlighted that the addition of nanoparticles into the TEOS matrix noticeably decreases the cracking during the drying phase.

Addition of TiO_2 nanoparticles, with antifouling and self-cleaning capabilities, seems a promising way in order to scale up the properties of TEOS based products; indeed titanium oxide properties have been widely tested in conservative treatments of stone surfaces (La Russa et al., 2012; Quagliarini et al., 2012, 2013; Kapridaki and Maravelaki-Kalaitzaki, 2013; Munafò et al., 2015; Gherardi et al., 2016; Xu et al., 2019). In the last years, self-cleaning and antifouling coatings have attracted the attention of many researchers in the field of stone conservation (Colangiuli et al., 2015; Lettieri et al., 2019). The self-cleaning properties of titanium oxide are due to its ability to photocatalyze the complete degradation of many organic contaminants and environmental toxins (Liu and Liu, 2016). Moreover, the photocatalytic activity of TiO_2 determines a collateral biocidal effect. The photocatalytic killing action by titania has been studied on a wide spectrum of organisms including bacteria, fungi, algae (Ruffolo et al., 2017). However, the structural properties of the target microorganism (e.g., the complexity and thickness of cell envelope) influence the microbiocidal efficacy of TiO_2: fungi, for instance, have a complex structure, which protects them from damage due to the radical species produced during the photocatalytic titania activities (Seven et al., 2004; Munafò et al., 2015).

In order to improve the antifouling effects, most coatings are prepared by dispersion of biocides molecules into the wet coating material (Omae, 2003; Almeida et al., 2007). This practice suffers from some drawbacks, such as poor control of the release rate of the antifoulants or degradation of the active substance. On the other hand, increasing the quantity of biocides into the coating, in order to extend its functionality over time is not economically, environmentally, and practically sustainable (Pinna et al., 2012; Fidanza and Caneva, 2019). Moreover, the high concentration of biocides into the coating may induce macroscopic damage of the film, detectable as a phase separation (Trojer et al., 2015).

Since several biocides are effective only for a short period of time after the application (between 6 months and 1 year), due to the cleaning of the surfaces after the treatments or due to the washing out of the compounds by rainfall, a frequent reapplication is needed (Jämsä et al., 2013). Thus, when indirect control methods are not possible (Almeida et al., 2007;

Caneva et al., 2008; Pinna et al., 2012; Fidanza and Caneva, 2019), improving the performance of the antifouling coating is necessary from both economical and environmental points of view.

Several biocides have been used in antifouling treatments for buildings conservation (Nugari and Salvadori, 2003; Caneva and Tescari, 2017; Pinna, 2017). A lot of active principles widely used in the past, such as organ-stannic or organotin compounds, have been excluded for toxicological reasons. The quaternary ammonium salts (Quats, e.g., benzalkonium chloride) are among the most used materials, despite their lower efficacy with respect others (Nugari and Salvadori, 2003; Caneva and Tescari, 2017; Pinna, 2017). Considering its chemical properties and the documented efficacy, we selected, as an active principle, 2-mercaptobenziothiazole (MBT), which can be easily encapsulated into silica based nanocapsules (Maia et al., 2015). In commercial products (e.g., Vancide 51, Vanderbilt Company) MBT is included in combination with dimethyldithiocarbamate (Nugari and Salvadori, 2003). Nevertheless, in order to improve the stability of our silica nanocontainers, we have encapsulated and confined only the 2-mercaptobenziothiazole (Ruggiero et al., 2019). The potential oxidation of the biocide induced by the TiO_2 nanoparticles is expected to decrease thanks to the confinement into the silica containers that "protect" the biocide against oxidation. In this contest, we tested the addition of two different kinds of nanofillers: the commercial TiO_2 nanoparticles and, for the first time, the silica nanocontainers (Si-NC and Si-MNP) loaded with MBT synthesized in our laboratory. The addition of these nanofillers to the TEOS-based coating formulation will improve the physic-chemical properties of the proposed product while providing a multifunctional composite coating with antifouling and self-cleaning properties.

In particular, TiO_2 nanoparticles provide self-cleaning properties, while the two silica nanocontainers (hereafter labeled as Si-NC and Si-MNP) loaded with 2-mercaptobenzothiazole (MBT) will contribute to the antifouling action through a controlled release of the biocide. The first silica nanocontainer (Si-NC) shows a core-shell structure, and thus is called NanoCapsule. The second one (Si-MNP) consists instead of Mesostructured NanoParticles. Si-NC and Si-MNP nanocontainers have different size and different textural properties, which affect the loading capability and, consequently, the release rate of the MBT, as measured in water for 120 days (Ruggiero et al., 2019).

This study presents the design and the characterization of a composite coating, which may have application on outdoor stone monuments, while planning the necessary further tests on different lithotypes and biological communities. The incorporation of TiO_2 and SiO_2 nanocontainers into coating matrices is supposed to increase the quality of a multifunctional composite coating, as it combines the self-cleaning and antibacterial properties of TiO_2, the antifouling and mechanical strength of SiO_2 nanocontainers, and the controlled release of the encapsulated biocide. In order to select the best composition from a physic-chemical point of view, we compare a series of coatings by mixing in the starting sols different concentrations of nanoparticles.

TABLE 1 | Contents of nanoparticles, expressed in percent volume of TEOS, in the multifunctional coatings.

Coatings	Nanoparticles		
	TiO$_2$	SiO$_2$	
		NC	MNP
C			
C_1%Si-NC		0.1%	
C_2%Si-NC		0.2%	
C_TiO$_2$/Si-NC	0.05%	0.05%	
C_2_TiO$_2$/Si-NC	0.1%	0.1%	
C_1%_Si-MNP			0.1%
C_2%_Si-MNP			0.2%
C_TiO$_2$/Si-MNP	0.05%		0.05%
C_2_TiO$_2$/Si-MNP	0.1%		0.1%

MATERIALS AND METHODS

In order to overcome the drawbacks of cracking of conventional TEOS-based materials, the proposed coatings was synthesized by combining three different strategies: (i) the addition of nanofillers, (ii) the addition of an non-ionic surfactant (n-octylamina) (González-Rivera et al., 2018), (iii) the modification of the elastic properties of the gel with Poly(dimethylsiloxane) hydroxy terminated (PDMS-OH) (Tamayo and Rubio, 2010; Zhang et al., 2010).

Preparation of Coatings

The coating matrix has been prepared as described in a recent article (Xu et al., 2012). In short, a typical starting sol has been prepared by mixing TEOS with ethanol, then different amounts of the two nanoparticles have been added, as summarized in **Table 1**. Technical grade TiO$_2$ (by Sigma-Aldrich), with an average particle size of ~21 nm, has been used as a photocatalytic element into the proposed coating. Two different SiO$_2$ nanocontainers (Si-NC and Si-MNP), synthesized in our laboratory, have been loaded with the 2-mercaptobenzothiazole (MBT, Sigma-Aldrich) and added to the coatings as antifouling agent. As reported in our previous work (Ruggiero et al., 2019), the Si-NC are core-shell structures with porous surface and a diameter of (128 ± 15) nm, while Si-MNP are mesoporous spherical nanoparticles with a diameter of (39 ± 4) nm.

In detail, the mixtures of TEOS and ethanol have been magnetically stirred (350 rpm) for 2 h at room conditions, prior to addition of the fillers (TiO$_2$ and Si-NC or Si-MNP). Afterwards, distilled water and PDMS-OH have been added under vigorous stirring (500 rpm). After 2 min of magnetic stirring, the mixture has been sonicated for 10 min. The n-octylamine has been added to each sol and the mixture has been magnetically stirred for further 20 min. The mole ratios of each mixture are 1 TEOS/16 ETOH/10H$_2$O/0.04 PDMS-OH/0.004 n-octylamine. TEOS (analytical grade reagent), n-octylamine and PDMS-OH (Mn = 550) have

been purchased from Sigma-Aldrich and used without further purification.

After completing the synthesis, 500 µL of each sol has been cast in plastic Petri dishes of 1.7 cm diameter and 0.7 cm height. Dried xerogels have been obtained by simple exposure of the sols to laboratory conditions (T = 25°C and RH = 60%). The xerogels are labeled according to **Table 1**.

Preparation of Colloidal Silica Nanofillers: Si-NC and Si-MNP

The silica nanocapsules (Si-NC) have been synthesized through the dynamic self-assembly of TEOS and CTAB (Ruggiero et al., 2018, 2019, 2020). After the dissolution of the cationic surfactant (CTAB) in deionized water, an ammonia aqueous solution (25–28% V) has been added. Then, the biocide (MBT) has been dissolved in the organic solvent (diethyl ether) and this second solution has been mixed to the aqueous solution under constant magnetic stirring. Once the miniemulsion stabilized, 2 mL of TEOS have been slowly dripped. The reaction has proceeded at room temperature for 24 h (Ruggiero et al., 2019). The obtained product has been finally filtered under vacuum, repeatedly washed and dried at laboratory conditions.

The silica nanoparticles (Si-MNP) have been obtained starting from the sonication of the CTAB water solution and MBT for 30 min. At the same time, 100 mL of deionized water have been basified by NaOH aqueous solution (2.0 M) and then added to the first solution. After reaching the temperature of 80°C, the silica precursor (TEOS = 1.25 mL) has been dripped and the final mixture is kept under fast stirring for an additional 2 h. Finally, the Si-MNP have been filtrated and washed several times with water (Knezevic et al., 2017; Ruggiero et al., 2019).
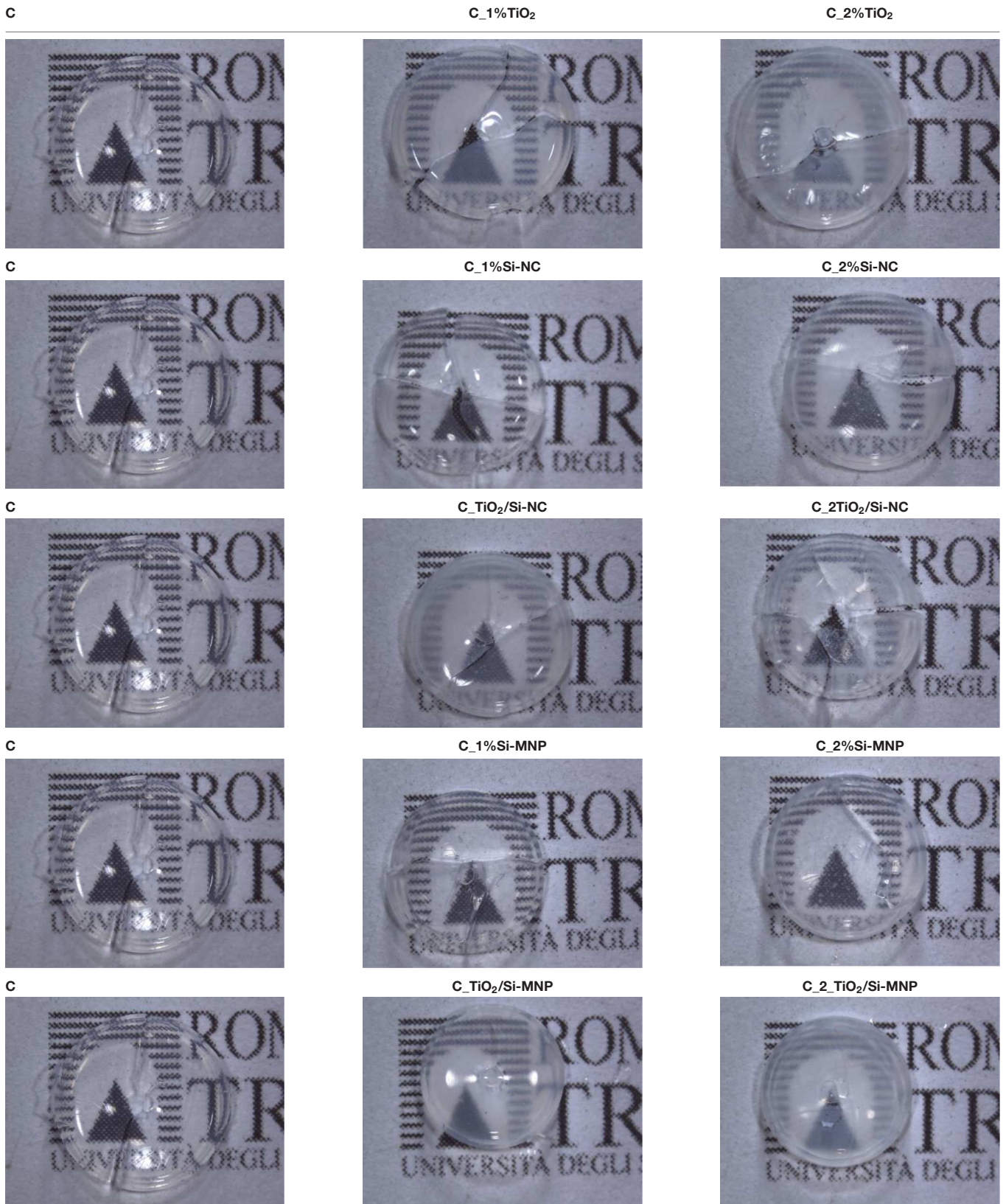
Characterization Procedures

The morphology of the nanosystems has been visualized by using a Field Emission Scanning Electron Microscope (FE-SEM, Sigma 300, Carl Zeiss SMT). Before the measurements, each sample has been sputtered with a thin layer of gold.
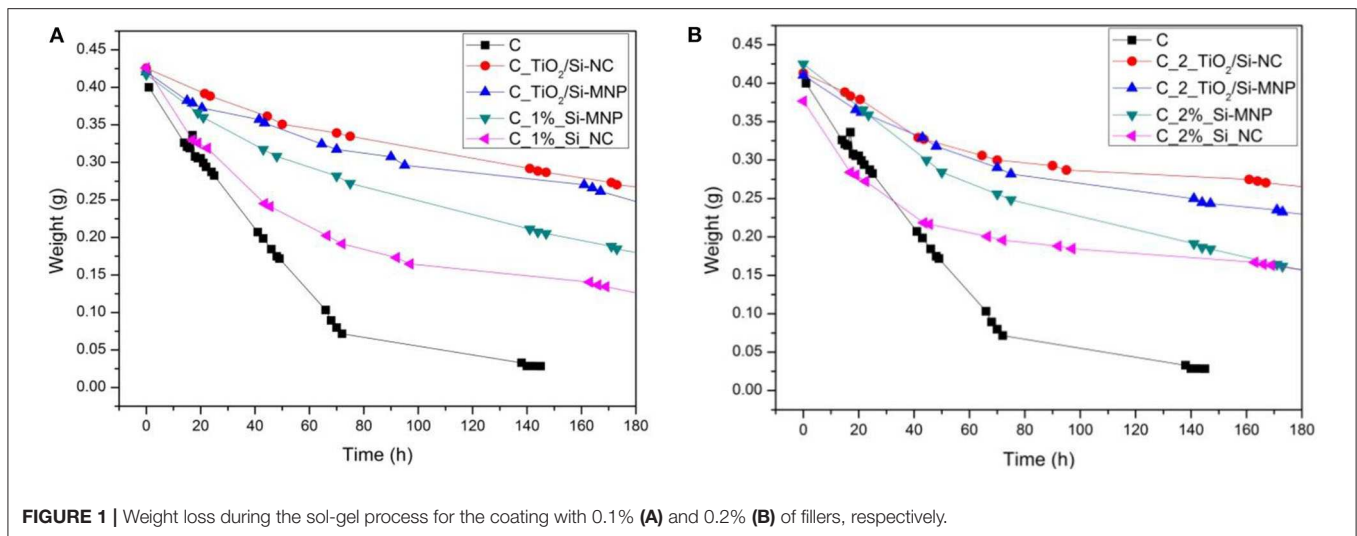
The BET surface area, the pore volume and pore size distribution have been characterized by the Nitrogen Physisoption at −196°C (Micromeritics Gemini V apparatus). Prior to the N$_2$ adsorption, the sample has been degassed in flowing He at 150°C by using a Micromeritics Flow Prep accessory.

The infrared (IR) spectra of the coatings have been collected using a ThermoFisher Nicolet iS50 FTIR instrument in Attenuated Total Reflection (ATR) mode. The spectra were recorded, on the powdered samples, from 4,000 to 400 cm^{-1} at 4 cm^{-1} of resolution; 132 scans have been recorded.

Possible changes in the color of each coating, over time, were evaluated by using a solid reflection spectrophotometer (Chroma-Meter CR-200 Konica Minolta), working with the illuminant D65 and the observer at 2°. For each coating, three spot areas were analyzed and each spot area was measured in triplicate. CIE L*a*b* color space has been used and the variations of color have been quantified by the total color difference ΔE^*, defined as: $\Delta E^* = \sqrt{\Delta L^{*2} + \Delta a^{*2} + \Delta b^{*2}}$.

TABLE 2 | Hybrid coatings after drying under laboratory conditions for different concentration of Si-NC/Si-MNP and TiO$_2$.

C	C_1%TiO$_2$	C_2%TiO$_2$

C	C_1%Si-NC	C_2%Si-NC

C	C_TiO$_2$/Si-NC	C_2TiO$_2$/Si-NC

C	C_1%Si-MNP	C_2%Si-MNP

C	C_TiO$_2$/Si-MNP	C_2_TiO$_2$/Si-MNP

FIGURE 1 | Weight loss during the sol-gel process for the coating with 0.1% **(A)** and 0.2% **(B)** of fillers, respectively.

RESULTS AND DISCUSSION

The coatings have been cast on plastic Petri dishes and examined after drying. First of all, their transparency has been investigated. Within the series shown in **Table 2**, dry coating (C) without nanoparticles is colorless and transparent but presents cracks. The addition of nanofillers into the sol changes the chromaticity of the final coatings: we notice a whitening of the charged coatings, with intensity depending on the type of nanoparticle and on their concentration. In particular, the addition of TiO_2 nanoparticles induces a whitening of the coatings with decreased transparency (first raw of **Table 2**). The coatings with Si-MNP maintains a good level of transparency with a few cracks. From the optical point of view, the reasonable amount of nanoparticles is 0.1% (w/v) and the best systems seem to be the coatings added with Si-MNP. The smaller size of Si-MNP in comparison with Si-NC allows the dispersion of these nanofillers into the coating matrix, reducing the optical effects correlated with the formation of aggregates.

In order to evaluate the effect of the nanofillers on the drying time of the gel, the weight loss of each sample has been measured. **Figures 1A,B** show the weight loss for the sols obtained by the addition of 0.1 and 0.2% w/v nanoparticles, respectively, over time (from 0 to 180 h), showing different drying rates.

The sample without nanoparticles shows the faster drying rate: the weight reaches a plateau after 145 h. Generally, the addition of the nanofillers slows down noticeably the drying rate, indeed the coatings with 0.2% w/v of fillers show a lower weight loss than the coatings with 0.1% w/v of fillers.

Comparing the green and magenta curves in **Figures 1A,B**, we notice that the coating charged with the Si-NC has a faster drying rate compared to that charged with the smaller sized Si-MNP. This difference persists, although reduced, when also TiO_2 particles are added; moreover, the presence of TiO_2 particles makes the drying process even slower. These observations, in the light of what reported in the previous paragraph, suggest that the nanoparticles are stratified in the coating, according to

their average dimension, with the Si-NC occupying the bottom layers of it. As a matter of fact, it can be verified by naked eye that the Si-NC tend to deposit at the bottom of the coating and thus have a limited effect on the drying rate. On the contrary, the TiO_2 and/or Si-MNP, characterized by a smaller size than the Si-NC, seem to be more homogeneously dispersed in the coatings. This implies a slowing of the evaporation of the solvents and, consequently, a longer drying time of the coating. The presence of the nanofillers, distributed into the thickness of the coating, hinders this evaporation process by slowing the gelation and, consequently, the drying of the products. These results suggest that nanofillers interfere with the drying process. The coatings in this way penetrate into the porous substrate before the viscosity naturally increases upon the sol-gel transition (Milani et al., 2007). The most promising system seems to be once again the C_TiO_2/Si-MNP.

SEM micrographs, collected with InLens detector on the upper surface of the coating, are compared in **Table 3**. All the coatings show a homogeneous morphology, consisting of microstructured folds, formed by uniform nanospheres of size of the order of 13–15 nm. These spherical microstructures do not depend on the size distribution and the morphology of the nanofillers. The SEM micrographs are quite similar one to each other and suggest that, during the deposition of the coatings into the petri dish, the nanofillers are preferably distributed through the thickness, or in some cases precipitate at the bottom and for these reasons are not visible on the surface.

In order to investigate the textural properties of the hybrid coatings, we have measured the N_2 adsorption-desorption isotherms of the most promising samples as the as far as the optical properties and drying rates are concerned, i.e., those containing 0.1% w/v of nanoparticles. The corresponding textural data are reported in **Table 4**.

All the analyzed coatings show type IV adsorption isotherms, with a H1 hysteresis loop (see **Figure 2A**). This loop is more evident for the coatings loaded with TiO_2 nanoparticles. These isotherm profiles suggest that the proposed coatings are a

TABLE 3 | SEM micrographs at different magnification of the samples added with silica nanoparticles and silica nanoparticles and TiO$_2$.

Sample	100 000 x	220 000 x
C_1%_Si-NC		
C_2%_Si-NC		
C_TiO$_2$/Si-NC		
C_2_TiO$_2$/Si-NC		
C_1%_Si-MNP		

(Continued)

TABLE 3 | Continued
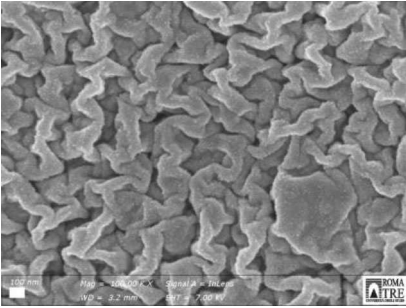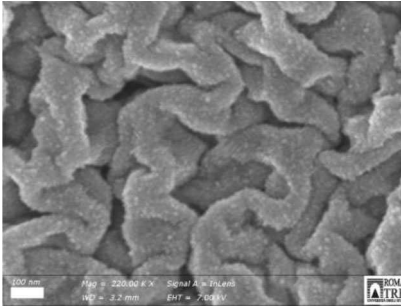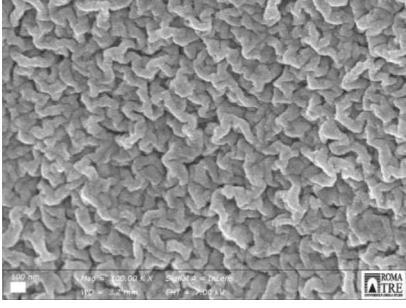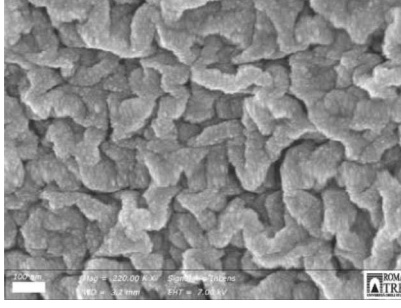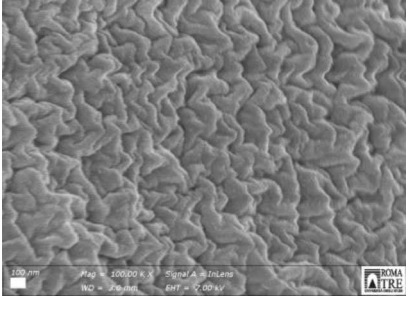
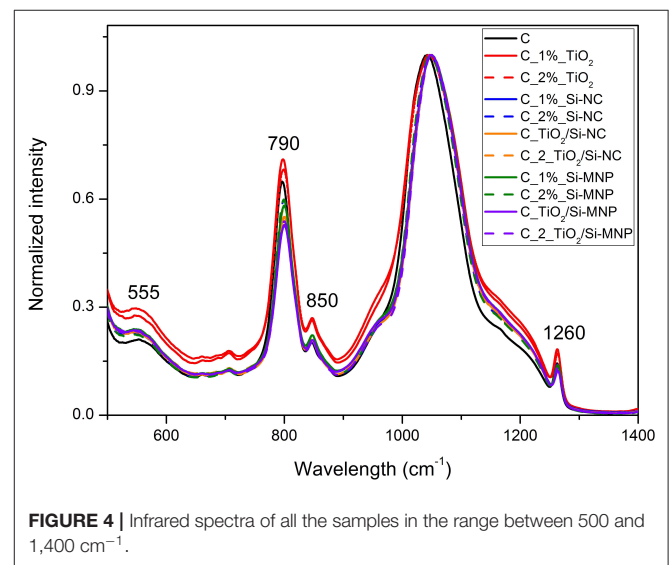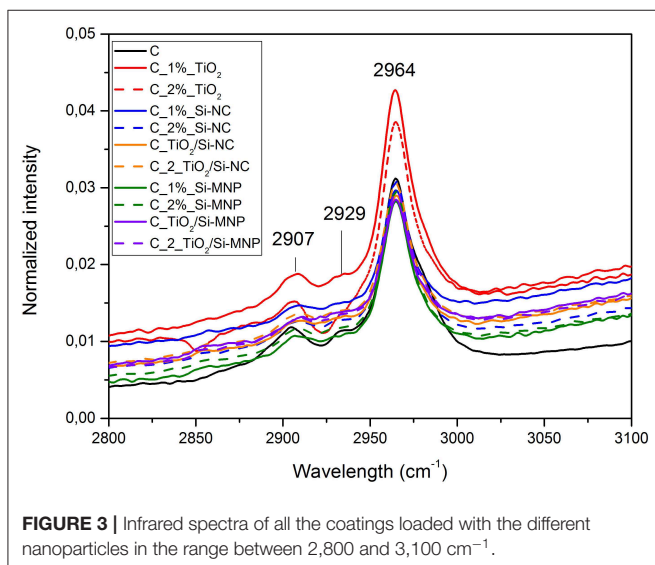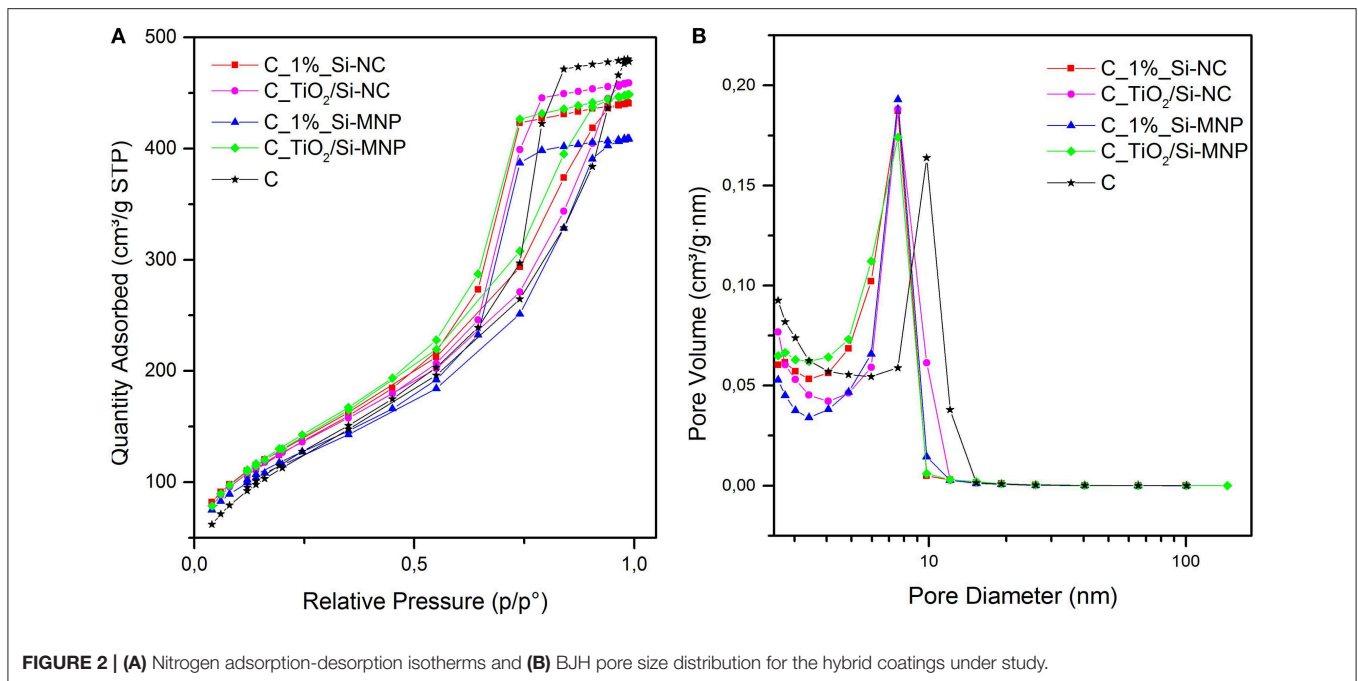| Sample	100 000 x	220 000 x
C_2%_Si-MNP		
C_TiO$_2$/Si-MNP		
C_2_TiO$_2$/Si-MNP		-

TABLE 4 | Surface area (S.A.), total pore volume (BJH P.V.), and pore size (BJH P.S.) of samples added with 0.1% of nanoparticles.

Sample	S.A (m^2g^{-1})	BJH P.V. (cm^3g^{-1})	BJH P.S. $P/P^0 < 0.60$ (nm)
C	440	0.70	8.4
C_1%Si-NC	481	0.75	5.9
C_1%_Si-MNP	475	0.76	6.4
C_1%_TiO$_2$/Si-NC	489	0.67	6.3
C_1%_TiO$_2$/Si-MNP	488	0.76	5.8

network of silica nanoparticles and that the fillers (Si-NC/Si-MNP and TiO$_2$) are embedded and integrated into the porous structures (Milani et al., 2007).

The BET surface area of the empty coating is 440 m^2g^{-1}, whereas for all sample with the addition of silica nanodevices and/or TiO$_2$ nanoparticles, the BET surface area is around 480 m^2g^{-1}. In **Figure 2B** the peak of sample C is centered at 8.4 nm (BJH P.S.): the addition of Si-NC/Si-MNP and/or

TiO$_2$ reduces the pore size to a value between 5.8 and 6.4 nm, without substantially changing the total pore volume (0.67 ÷ 0.76 cm^3g^{-1}). These results suggest that the nanoparticles are integrated into the coating matrix, inducing an increase of BET surface area of about 10% and a decrease of the pore size of about 30% in comparison with the empty coating (C). The textural properties outline that the size of the two different silica fillers determines the properties of the coatings. When the TiO$_2$ nanoparticles are added into the coating formulations, the differences in surface area between the coating loaded with Si-NC and Si-MNP are reduced, as shown in **Table 4**. Moreover, TiO$_2$ nanoparticles induce an increase of the pore size in the coating loaded with Si-NC. This behavior suggests that the TiO$_2$ nanoparticles work in synergy with the Si-NC, positively shaping the network structure. The Si-NC, because of their diameter, tend to precipitate and agglomerate during the sol-gel process. Otherwise, the Si-MNP shape the network modifying the porosity of the coating in comparison with the empty coating. For this reason, when the TiO$_2$ nanoparticles are added to the coating with Si-MNP, the TiO$_2$ is embedded in the porosity created by the

FIGURE 2 | (A) Nitrogen adsorption-desorption isotherms and **(B)** BJH pore size distribution for the hybrid coatings under study.

FIGURE 3 | Infrared spectra of all the coatings loaded with the different nanoparticles in the range between 2,800 and 3,100 cm^{-1}.

FIGURE 4 | Infrared spectra of all the samples in the range between 500 and 1,400 cm^{-1}.

Si-MNP, decreasing the pore diameter of the C_ TiO$_2$/Si-MNP (Pinho and Mosquera, 2011).

Structural characterization of dried coatings has been performed by means of Fourier Transformed Infrared Spectroscopy. **Figures 3–5** report the FTIR spectra of the coatings under study. The band corresponding to the Si–O–Si vibration ($\sim$1,050 cm^{-1}), being the most intense, has been used for the normalization of the infrared spectra. The spectra (**Figure 3**) show a few bands that are unequivocally assigned to vibrations of an organic fraction, namely PDMS-OH. In particular, the band at 2,907 cm^{-1} corresponds to the symmetric stretching vibration of the C-H bonds, whereas the bands at

2,929 and 2,964 cm^{-1} are assigned to the asymmetric stretching vibration of the C-H bonds in CH$_2$ and CH$_3$ groups, respectively (Tamayo and Rubio, 2010; González-Rivera et al., 2018).

The symmetric bending vibration of CH$_3$ groups in PDMS-OH contributes to a sharp band centered around 1,260 cm^{-1} (Zhang et al., 2010; Goffredo et al., 2019) in **Figure 4**. The band at $\sim$790 cm^{-1} is related to the rocking modes of methyl groups and to the Si-C stretching in Si-(CH$_3$)$_n$, as reported in **Figure 4** (Fidalgo et al., 2005; Johnson et al., 2013).

The copolymerization of Si-OH group of hydrolyzed TEOS and Si-OH of PDMS-OH is suggested by the band at 850 cm^{-1} (Tellez et al., 2003), as reported in **Figure 4**. This implies that
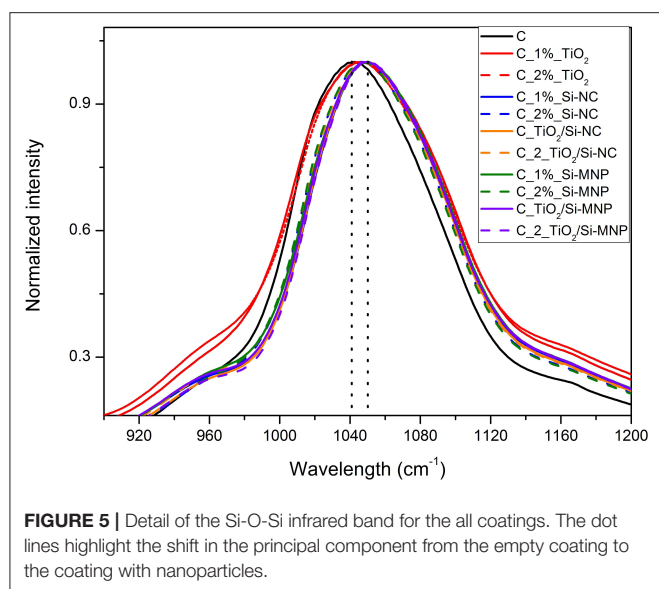
FIGURE 5 | Detail of the Si-O-Si infrared band for the all coatings. The dot lines highlight the shift in the principal component from the empty coating to the coating with nanoparticles.

TABLE 5 | Shift and assignments of the bands observed in the spectra of the coatings.

Sample	δ Si-O-Si in SiO$_4$ (nm)	ν_{as} Si-O-Si in SiO$_4$ and SiO$_6$ (nm)
C	555	1,042
C_1%_TiO$_2$	550	1,046
C_2%_TiO$_2$	552	1,047
C_1%_Si-NC	550	1,046
C_2%_Si-NC	550	1,050
C_TiO$_2$/Si-NC	543	1,050
C_2_TiO$_2$/Si-NC	549	1,050
C_1%_Si-MNP	550	1,046
C_2%_Si-MNP	552	1,050
C_TiO$_2$/Si-MNP	550	1,048
C_2_TiO$_2$/Si-MNP	552	1,051

during the synthesis PDMS-OH and TEOS interact, producing a homogeneous hybrid coating.

Several vibration modes of siloxane bonds contribute to the most intense band of the infrared spectra, in the region between 1,000 and 1,250 cm^{-1}. In detail, the large band centered at 1,050 cm^{-1} is related to the asymmetric ν(Si–O–Si) stretching of the Si-O-Si network and it can be deconvoluted in four components: two longitudinal (LO) and two transverse (TO) optic modes. These components correspond to the four-membered (SiO)$_4$ and the six-membered (SiO)$_6$ arrangement of siloxane rings (Fidalgo and Ilharco, 2004). The position and the relative intensities of the LO and TO modes, according to the literature, change when chemical groups or organic molecules modify the silica network (Fidalgo and Ilharco, 2004).

In this contest, a shift of the Si-O-Si asymmetric stretching bands toward higher wavelengths in comparison with the empty coating is observed (from 1,042 to $\sim$1,050 cm^{-1}, **Figure 5**). These shifts are ascribed to the network deformation needed to accommodate the nanoparticles within the hybrid coating

matrix, as summarized in **Table 5**. This phenomenology outlines that the distance between interacting species (e.g., the matrix and the nanoparticles) is reduced by the increase of the long-range Coulomb interactions. This finding is in agreement with the porosity decrease, suggested by N$_2$ adsorption-desorption measurements (Li et al., 2013; Xu and Li, 2013).

As reported in **Table 5**, the position of the band at $\sim$555 cm^{-1} (**Figure 4**), assigned to a coupled mode in four-member siloxane rings (SiO)$_4$, moves from a maximum of 555 cm^{-1} to a minimum of 543 cm^{-1}, depending on the species and concentration of dispersed nanoparticles (Tamayo and Rubio, 2010).

In order to evaluate the chromatic stability of the coating over time, the total color variation (ΔE^*) of the samples has been measured at $t = 0$[1] and after 20, 40, and 60 days. All the coatings show a ΔE^* below the perceivable threshold. The chromatic feature of the coating does not change over time, regardless of the type and quantity of nanoparticles added as filler. Such absence of chromatic variation will be further tested in direct application of these coatings on outdoor building surfaces, following the standards in the field. Future plans also include investigating the photocatalytic activity of the commercial TiO$_2$ nanoparticles added to the coating, and the long-time effects on the stone properties after the treatment (e.g., color, porosity, and permeability changes).

CONCLUSIONS

In this work, we report the synthesis and the multi-analytical characterization of an innovative TEOS-based composite coating with the addition of two different silica nanofillers with antifouling properties. The best results in terms of optical properties (e.g., visual aspect and transparency), porosity and absence of cracking are obtained with the following nanofiller concentrations: 0.05% w/v of TiO$_2$ and 0.05% w/v of Si-MNP or Si-NC loaded with MBT. The coatings with Si-MNP as filler show better properties than the coatings with Si-NC: indeed, the size of the filler shapes the behavior of the coatings, modifying not only the visual aspect, but also the drying rate. Further tests are in progress to check the interaction of this new coating with the most common substrates of interest for conservation of buildings and Cultural Heritage, as for instance its photocatalytic and biocidal activities and long-lasting efficacy on different lithotypes.

DATA AVAILABILITY STATEMENT

The datasets generated for this study are available on request to the corresponding author.

AUTHOR CONTRIBUTIONS

LR made the synthesis, some characterizations, and drafted the manuscript. MI and LT made FT-IR analysis. MF made the colorimetric measurements. GC, MR, and AS coordinated the project and participated in the discussion of the results.

---

[1]It has been considered as time 0, when the coating reached a constant weight.

All authors contributed to write the article and approved the submitted version.

REFERENCES

Almeida, E., Diamantino, T. C., and De Sousa, O. (2007). Marine paints: The particular case of antifouling paints. *Prog. Org. Coat.* 59:2. doi: 10.1016/j.porgcoat.2007.01.017

Angulo-Olais, R., Illescas, J. F., Aguilar-Pliego, J., Vargas, C. A., and Haro-Pérez, C. (2018). Gel point determination of TEOS-based polymeric materials with application on conservation of cultural heritage buildings. *Adv. Condens. Matter Phys.* 2018:5784352. doi: 10.1155/2018/5784352

Bourges, A., Fehr, K. T., Simon, S., and Snethlage, R. (2008). Correlation between the micro-structure and the macroscopic behaviour of sandstones. *Restor. Build. Monum. Int. J.* 14, 157–166. doi: 10.1515/rbm-2008-6214

Caneva, G., Nugari, M. P., and Salvadori, O. (2008). *Plant Biology for Cultural Heritage.* Los Angeles, CA: Getty Conservation Institute.

Caneva, G., and Tescari, M. (2017). "Stone biodeterioration: treatments and preventive conservation," in *Proceedings of International Symposium of Stone Conservation, Conservation Technologies for Stone Cultural Heritages: Status and Future Prospects* (Seoul).

Colangiuli, D., Calia, A., and Bianco, N. (2015). Novel multifunctional coatings with photocatalytic and hydrophobic properties for the preservation of the stone building heritage. *Constr. Build. Mater.* 93, 189–196 doi: 10.1016/j.conbuildmat.2015.05.100

Doehne, E., and Price Clifford, A. (2010). *Stone Conservation: An Overview of Current Research.* Technical Report. Getty Conservation Institute, Los Angeles, CA.

Fidalgo, A., Ciriminna, R., Ilharco, L. M., and Pagliaro, M. (2005). Role of the alkyl-alkoxide precursor on the structure and catalytic properties of hybrid sol-gel catalysts. *Chem. Mater.* 17, 6686–6694. doi: 10.1021/cm051954x

Fidalgo, A., and Ilharco, L. M. (2004). Chemical tailoring of porous silica xerogels: local structure by vibrational spectroscopy. *Chem. Eur. J.* 10, 392–398. doi: 10.1002/chem.200305079

Fidanza, M. R., and Caneva, G. (2019). Natural biocides for the conservation of stone cultural heritage: a review. *J. Cult. Herit.* 38, 271–286. doi: 10.1016/j.culher.2019.01.005

Gherardi, F., Colombo, A., D'Arienzo, M., Di Credico, B., Goidanich, S., Morazzoni, F., et al. (2016). Efficient self-cleaning treatments for built heritage based on highly photo-active and well-dispersible TiO$_2$ nanocrystals. *Microchem. J.* 126, 54–62. doi: 10.1016/j.microc.2015.11.043

Goffredo, G. B., Accoroni, S., and Totti, C. (2019). "Nanotreatments to inhibit microalgal fouling on building stone surfaces," in *Nanotechnology in Eco-efficient Construction, 2nd Edn* (Woodhead Publishing), 619–647. doi: 10.1016/B978-0-08-102641-0.00025-6

González-Rivera, J., Iglio, R., Barillaro, G., Duce, C., and Tinè, M. R. (2018). Structural and thermoanalytical characterization of 3D Porous PDMS foam materials: the effect of impurities derived from a sugar templating process. *Polymers* 10:616. doi: 10.3390/polym10060616

Illescas, J. F., and Mosquera, M. J. (2011). Surfactant-synthesized PDMS/silica nanomaterials improve robustness and stain resistance of carbonate stone. *J. Phys. Chem. C*, 115, 14624–14634. doi: 10.1021/jp203524p

Jackson, M. D., Marra, F., Hay, R. L., Cawood, C., and Winkler, E. M. (2005). The judicious selection and preservation of tuff and travertine building stone in ancient Rome. *Archaeometry* 47, 485–510. doi: 10.1111/j.1475-4754.2005.00215.x

Jämsä, S., Mahlberg, R., Holopainen, U., Ropponen, J., Savolainen, A., and Ritschkoff, A.-C. (2013). Slow release of a biocidal agent from polymeric microcapsules for preventing biodeterioration. *Progress Organic Coat.* 76, 269–276. doi: 10.1016/j.porgcoat.2012.09.018

Johnson, L. M., Gao, L., Shields, C. W., Smith, M., Efimenko, K., Cushing, K., et al. (2013). Elastomeric microparticles for acoustic mediated bioseparations. *J. Nanobiotechnol.* 11:22. doi: 10.1186/1477-3155-11-22

Kapridaki, C., and Maravelaki-Kalaitzaki, P. (2013). TiO$_2$-SiO$_2$-PDMS nano-composite hydrophobic coating with self-cleaning properties for marble protection. *Progress Organ. Coat.* 76, 400–410. doi: 10.1016/j.porgcoat.2012.10.006

Kim, E. K., Won, J., Do, J.-y., Kim, S. D., and Kang, Y. S. (2009). Effects of silica nanoparticle and GPTMS addition on TEOS-based stone consolidants. *J. Cult. Herit.* 10, 214–221. doi: 10.1016/j.culher.2008.07.008

Knezevic, N. Z., Mauriello Jimenez, C., Albino, M., Vukadinovic, A., Mrakovic, A., Illes, E., et al. (2017). Synthesis and characterization of core-shell magnetic mesoporous silica and organosilica nanostructures. *MRS Adv.* 2, 1037–1045. doi: 10.1557/adv.2017.69

La Russa, M. F., Ruffolo, S. A., Rovella, N., Belfiore, C. M., Palermo, A. M., Guzzi, M. T., et al. (2012). Multifunctional TiO$_2$ coatings for cultural heritage. *Prog. Org. Coat.* 74, 186–191. doi: 10.1016/j.porgcoat.2011.12.008

Lettieri, M., Colangiuli, D., Masieri, M., and Calia, A. (2019). Field performances of nanosized TiO$_2$ coated limestone for a self-cleaning building surface in an urban environment. *Build. Environ.* 147, 506–516. doi: 10.1016/j.buildenv.2018.10.037

Li, D., Xu, F., Liu, Z., Zhu, J., Zhang, Q., and Shao, L. (2013). The effect of adding PDMS-OH and silica nanoparticles on sol–gel properties and effectiveness in stone protection. *Appl. Surf. Sci.* 266, 368–374. doi: 10.1016/j.apsusc.2012.12.030

Liu, Y., and Liu, J. (2016). Design of multifunctional SiO$_2$-TiO$_2$ composite coating materials for outdoor sandstone conservation. *Ceramics Int.* 42, 13470–13475. doi: 10.1016/j.ceramint.2016.05.137

Maia, F., Silva, A. P., Fernandes, S., Cunha, A., Almeida, A., Tedim, J., et al. (2015). Incorporation of biocides in nanocapsules for protective coatings used in maritime applications. *Chem. Eng. J.* 270, 150–157. doi: 10.1016/j.cej.2015.01.076

McNamara, C. J., and Mitchell, R. (2005). Microbial deterioration of historic stone. *Front. Ecol. Environ.* 3, 445–451. doi: 10.1890/1540-9295(2005)003[0445:MDOHS]2.0.CO;2

Milani, C., Velo-Simpson, M. L., and Scherer, G. W. (2007). Particle-modified consolidants: a study on the effect of particles on sol-gel properties and consolidation effectiveness. *J. Cult. Herit.* 8, 1–6. doi: 10.1016/j.culher.2006.10.002

Mosquera, M. J., Bejarano, M., De la Rosa-Fox, N., and Esquivias, L. (2003). Producing crack-free colloid-polymer hybrid gels by tailoring porosity. *Langmuir* 19, 951–957. doi: 10.1021/la0265981

Munafò, P., Goffredo, G. B., and Quagliarini, E. (2015). TiO$_2$-based nanocoatings for preserving architectural stone surfaces: an overview. *Constr. Build. Mater.* 84, 201–218. doi: 10.1016/j.conbuildmat.2015.02.083

Nugari, M. P., and Salvadori, O. (2003). "Biocides and treatment of stone: limitations and future prospects," in *Art, Biology, and Conservation: Biodeterioration of Works of Art*, eds R. J. Koestler, V. H. Koestler, A. Elena Charola, and F. E. Nieto-Fernandez (New York, NY: The Metropolitan Museum of Art), 518–535.

Omae, I. (2003). General aspects of tin-free antifouling paints. *Chem. Rev.* 103:3431. doi: 10.1021/cr030669z

Pinho, L., Elhaddad, F., Facio, D. S., and Mosquera, M. J. (2013). A novel TiO$_2$-SiO$_2$ nanocomposite converts a very friable stone into a self-cleaning building material. *Appl. Surf. Sci.* 275, 389–396. doi: 10.1016/j.apsusc.2012.10.142

Pinho, L., and Mosquera, M. J. (2011). Titania-silica nanocomposite photocatalysts with application in stone self-cleaning. *J. Phys. Chem. C* 115, 22851–22862. doi: 10.1021/jp2074623

Pinna, D. (2017). *Coping With Biological Growth on Stone Heritage Objects: Methods, Products, Applications, and Perspectives*. New York, NY: Apple Academic Press.

Pinna, D., Salvadori, B., and Galeotti, M. (2012). Monitoring the performance of innovative and traditional biocides mixed with consolidants and water-repellents forthe prevention of biological growth on stone. *Sci. Total Environ.* 423, 132–141. doi: 10.1016/j.scitotenv.2012.02.012

Quagliarini, E., Bondioli, F., Goffredo, G. B., Licciulli, A., and Munafò, P. (2012). Smart surfaces for architectural heritage: preliminary results about the application of TiO₂-based coatings on travertine. *J. Cult. Herit.* 13, 204–209. doi: 10.1016/j.culher.2011.10.002

Quagliarini, E., Bondioli, F., Goffredo, G. B., Licciulli, A., and Munafò, P. (2013). Self-cleaning materials on architectural heritage: compatibility of photo-induced hydro-philicity of TiO₂ coatings on stone surfaces. *J. Cult. Herit.* 14, 1–7. doi: 10.1016/j.culher.2012.02.006

Ruffolo, S. A., De Leo, F., Ricca, M., Arcudi, A., Silvestri, C., Bruno, L., et al. (2017). Medium-term *in situ* experiment by using organic biocides and titanium dioxide for the mitigation of microbial colonization on stone surfaces. *Int. Biodeteriorat. Biodegrad.* 123, 17–26 doi: 10.1016/j.ibiod.2017.05.016

Ruggiero, L., Bartoli, F., Fidanza, M. R., Zurlo, F., Marconi, E., Gasperi, T., et al. (2020). Encapsulation of environmentally-friendly biocides in silica nanosystems for multifunctional coatings. *Appl. Surf. Sci.* 514:145908. doi: 10.1016/j.apsusc.2020.145908

Ruggiero, L., Crociani, L., Zendri, E., El Habra, N., and Guerriero, P. (2018). Incorporation of the zosteric sodium salt in silica nanocapsules: synthesis and characterization of new fillers for antifouling coatings. *Appl. Surf. Sci.* 439, 705–711. doi: 10.1016/j.apsusc.2017.12.228

Ruggiero, L., Di Bartolomeo, E., Gasperi, T., Luisetto, I., Talone, A., Zurlo, F., et al. (2019). Silica nanosystems for active antifouling protection: nanocapsules and mesoporous nanoparticles in controlled release applications. *J. Alloys Compd.* 798, 144–148. doi: 10.1016/j.jallcom.2019.05.215

Salazar-Hernández, C., Zárraga, R., Alonso, S., Sugita, S., Calixto, S., and Cervantes, J. (2009). Effect of solvent type on polycondensation of TEOS catalyzed by DBTL as used for stone consolidation. *J. Sol Gel Sci. Technol.* 49, 301–310. doi: 10.1007/s10971-008-1879-9

Scheerer, S., Ortega Morales, O., and Gaylarde, C. (2009). Microbial deterioration of stone monuments-an updated overview. *Adv Appl Microbiol.* 66, 97–139. doi: 10.1016/S0065-2164(08)00805-8

Seven, O., Dindar, B., Aydemir, S., Metin, D., Ozinel, M., and Icli, S. (2004). Solar photocatalytic disinfection of a group of bacteria and fungi aqueous suspensions with TiO₂, ZnO and Sahara Desert dust. *J. Photochem. Photobiol. Chem.* 165, 103–107. doi: 10.1016/j.jphotochem.2004.03.005

Tamayo, A., and Rubio, J. (2010). Structure modification by solvent addition into TEOS/PDMS hybrid materials. *J. Non Crystalline Solids* 356, 1742–1748. doi: 10.1016/j.jnoncrysol.2010.04.025

Tellez, L., Rubio, J., Rubio, F., Morales, E., and Oteo, J. L. (2003). Synthesis of inorganic-organic hybrid materials from TEOS, TBT and PDMS. *J. Mater. Sci.* 38:1773. doi: 10.1023/A:1023240129477

Torraca, G. (2009). *Lectures on Materials Science for Architectural Conservation*. Los Angeles, CA: Getty Conservation Institute.

Trojer, M. A., Nordstierna, L., Bergek, J., Blanckc, H., Holmberg, K., and Nydén, M. (2015). Use of microcapsules as controlled release devices for coatings. *Adv. Coll. Interface Sci.* 222, 18–43. doi: 10.1016/j.cis.2014.06.003

Wen, J., and Mark, J. E. (1995). Sol-Gel preparation of composites of poly(dimethylsiloxane) with SiO₂ and SiO₂/TiO₂, and their mechanical properties. *Polymer J.* 27, 492–502. doi: 10.1295/polymj.27.492

Xu, F., and Li, D. (2013). Effect of the addition of hydroxyl-terminated polydimethylsiloxane to TEOS-based stone protective materials. *J. Sol Gel Sci. Technol.* 65, 212–219. doi: 10.1007/s10971-012-2926-0

Xu, F., Li, D., Zhang, Q., Zhang, H., and Xu, J. (2012). Effects of addition of colloidal silica nanoparticles on TEOS-based stone protection using n-octylamine as catalyst. *Progress Organ. Coat.* 75, 429–434. doi: 10.1016/j.porgcoat.2012.07.001

Xu, F., Zeng, W., and Li, D. (2019). Recent advance in alkoxysilane-based consolidants for stone. *Progress Organ. Coat.* 127, 45–54. doi: 10.1016/j.porgcoat.2018.11.003

Zárraga, R., Cervantes, J., Salazar-Hernandez, C., and Wheeler, G. (2010). Effect of the addition of hydroxyl-terminated polydimethylsiloxane to TEOS-based stone consolidants. *J. Cult. Heritage* 11, 138–144. doi: 10.1016/j.culher.2009.07.002

Zhang, X., Ye, H., Xiao, B., Yan, L., and Jiang, B. (2010). Sol–Gel preparation of PDMS/silica hybrid antireflective coatings with controlled thickness and durable antireflective performance. *J. Phys. Chem. C* 114, 19979–19983. doi: 10.1021/jp106192z